International Conference on Space Optics—ICSO 2008

Toulouse, France

14–17 October 2008

Edited by Josiane Costeraste, Errico Armandillo, and Nikos Karafolas

A variable-tune spatial heterodyne spectrometer for broadband spectral line studies in the visible and near-UV

Olivia R. Dawson

Walter M. Harris

International Conference on Space Optics — ICSO 2008, edited by Josiane Costeraste, Errico Armandillo, Nikos Karafolas, Proc. of SPIE Vol. 10566, 105662D · © 2008 ESA and CNES
CCC code: 0277-786X/17/$18 · doi: 10.1117/12.2308254

A VARIABLE-TUNE SPATIAL HETERODYNE SPECTROMETER FOR BROADBAND SPECTRAL LINE STUDIES IN THE VISIBLE AND NEAR-UV

Olivia R. Dawson[(1)], Walter M. Harris[(2)]

[(1)]Dept. of Earth & Space Sciences, University of Washington Seattle, WA 98195 USA, E-mail: ord@u.washington.edu.
[(2)]University of California-Davis, Department of Applied Science, One Shields Ave., Davis, CA 95616 USA, E-mail: wmharris@ucdavis.edu.

ABSTRACT

Reflective Spatial Heterodyne Spectroscopy (SHS) is an interferometric technique that combines high resolving power and a large input acceptance angle in a format that is compact enough for use at small telescope focal planes and in spacecraft observations of targets in the visible to far ultra-violet (FUV) spectral range. SHS instruments are well suited to the study of faint, extended emission line sources, particularly in the UV where stellar background continuum becomes weak. Their primary limitation comes from the limited spatial sampling of the output interference pattern generated by the incoming spectral source, which limits their use to narrow bandpass near the central tuning wavelength. We describe a the first light results from a broadband SHS that can be used to scan the tuning wavelength across a bandpass extending from 300 to 700 nm. The limitations on the bandpass are arbitrary and can easily be extended into the UV or near infrared. We discuss the results of these validation program and the potential improvements that could be used to expand and/or improve the broadband spectral response of the instrument.

1 INTRODUCTION

Spectral observations of the intensity and distribution of UV-Visible emission/absorption features has become a staple technique for the remote sensing of faint, extended targets including comets, the interstellar medium, planetary upper atmospheres and their near space ion/neutral environments, and the heliopshere. In addition to their intensity and spatial extent, the line shapes and ratios of these emission features further contain a plethora of useful information about velocity distributions, thermal (and non-thermal) properties, turbulence, radiative transfer effects, isotopic ratios and contributions from multiple sources (background emission, coronae, etc.). Extension of spectral studies into the UV magnifies the available information by eliminating solar continuum radiation for solar system targets and background stellar continuum for astrophysical targets.

A variety of instruments have been developed over the past several decades to study emission line features from Earth-orbit remote sensing (HST, SOHO, FUSE, IUE, etc.) and remote *in situ* (Galileo, Cassini, Rosetta, Image, Voyager, etc.) platforms. For the most part, these instruments have been either narrow bandpass filter imagers or variations of a grating spectrograph. Their performance may be coarsely broken down to instruments with large effective area (A_{eff}) that emphasize spectral or spatial resolution (e.g. HST-STIS) and those with large étendue (A_{eff} x FOV) that emphasize sensitivity and photometric accuracy (e.g. Cassini UVIS; Rosetta ALICE). In addition to these, the technique of field summing interference spectroscopy has demonstrated a significant utility to these studies by providing a third class of instrument, one that combines large étendue with high spectral resolving power that is capable of discriminating the lower energy line shape structures that typify solar system targets. Instruments of this type, such as Fabry-Perot interferometers and Spatial heterodyne spectrometers (SHS) can offer improvements in sensitivity relative to grating spectrometers for extended targets of up to several orders of magnitude while having a modest input aperture and a compact format that makes them suitable for a wide variety of applications where weight and volume resources are at a premium.

A limitation of interference spectroscopy is the bandpass over which the instruments may be used. Fabry-Perot interferometers are limited in a single configuration to the free spectral range dividing individual orders and, in the case of scanning, multiple etalon systems, by the range over which the conditions between the plates (e.g. distance or index of refraction) may be changed. Michelson style Fourier transform spectrometers can be tuned over an arbitrarily large spectral range, but such instruments tend to be larger and their optical tolerances are difficult to maintain over large translations of their scanning mirrors, particularly for all reflective systems that can operate in the far UV [1]. The recent advent of beamsplit [2,3,4,5] and all-reflective [6,7] has opened a middle ground of providing a combination of modest bandpass and high resolving power (R~50000-100000), over a large field

of view (FOV). While a SHS is optically similar a FTS, it samples spectra in the spatial rather than temporal domain and does so without the requirement of a translating mirror. Like FTS instruments, SHS instruments are theoretically capable of sampling an arbitrarily large bandpass, but in practice they are limited by the format of the detector being used to sample the input spectrum. Typical implementations are able to sample a range extending at most to a few percent of central wavelength of its bandpass (bpass/λ_c~0.01).

In this paper we discuss the results of our effort to construct and validate a broadband implementation of the SHS that retains its advantages of compact format and high resolving power. Our design is based on an all-reflective format, similar in basic design to a Sagnac interferometer, that is suitable for use at wavelengths in far or extreme UV. To achieve broadband performance we adopt the strategy of scanning the tuning wavelength of the interferometer by rotating the pilot flat mirrors that guide the two interfering beams through the system. In effect this moves the acceptance bandpass of the optical system across the input spectrum. The resulting system is limited in wavelength only by the size of the pilot mirrors, the blaze characteristics of the grating, and the quantum efficiency profile of the detector used. Our prototype was built with a tunable range from 300 to 700 nm and optically coupled to the incoming beam of the West Auxiliary telescope of the McMath-Pierce observatory on Kitt Peak, where it was validated in June 2007. Here we will describe the all-reflective technique and the manner in which a SHS may be dynamically tuned. We will also provide the results of laboratory and field operations of the prototype and discuss various methods for improving the performance of later generation instruments.

2 THEORY of SHS

The most frequently used configuration of SHS is similar to a Twyman-Green Interferometer (TGI). The TGI (figure 1) is a special case of the better-known Michelson interferometer, where the input and output beams have been collimated and the mirrors have been set for constructive interference near zero optical path difference between the two arms. Tilting one of the mirrors in the TGI rotates the wavefronts of the two beams with respect to each other so that a series of fizeau (vertical) fringes are obtained at the output with a spatial frequency directly related to the angle of rotation (γ) and the wavenumber (σ) of the light. The effect is similar to a Young's slit experiment where the tilt of the mirror changes the separation of the two sources.

The SHS takes this concept further by replacing the two mirrors with gratings (figure 3.1b). The effect of using gratings in the TGI format is that the apparent tilt (θ) at a given wavenumber of the 'reflecting' surfaces in the interferometer becomes dependent on the dispersive properties of the grating, where

$$sin(\beta) = mN/\sigma - sin(\alpha) \qquad (1)$$

α and β are respectively the angles of incidence and diffraction relative the grating normal, m is the order of diffraction, and N is the number of groves/mm (figure). If the incident angle α is held constant, then the rotation of the wavefronts, and hence the spatial frequency of the fizeau fringes becomes entirely dependent on the wavenumber.

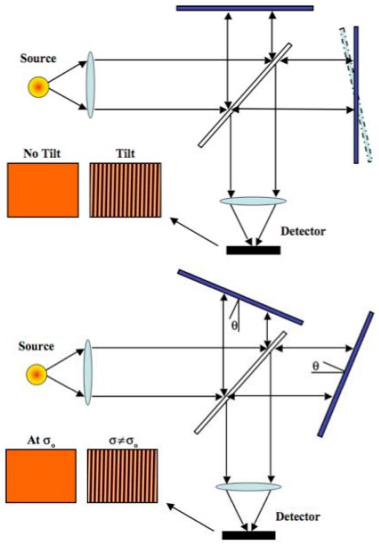

Fig. 1. A comparison of a Twyman-Green Interferometer (above) with the basic beamsplit SHS (below). Note that a relative rotation of the optical components (symmetric in the SHS) introduces a relative rotation of the wavefronts, leading to the output interference pattern.

Alignment of a SHS starts with a target wavenumber σ_o. The gratings are tilted by an angle θ corresponding to the Littrow ($\alpha = \beta$) configuration at σ_o such that the relative tilt (γ) of the reflected wavefronts is zero and the classical zero-path TGI configuration (figure 3.1b) is obtained. However, this condition holds <u>only</u> for σ_o. For *all* other wavelengths dispersion results in a net rotation angle γ between the wavefronts, such that they interfere at the output with a *monochromatic* spatial frequency [2,3] of

$$f_x = 2\sigma sin(\gamma) \sim 4(\sigma - \sigma_o)tan(\theta) \qquad (2)$$

Each input wavenumber will therefore produce a unique interference pattern at the output of the instrument, resulting in a superposition of fringes of different frequency and intensity. Herein lies the heterodyne aspect of the SHS: The instrument essentially

heterodynes the input spectral signature with the Littrow wavenumber of the gratings. All output frequencies are relative to σ_o. The combined pattern resulting from a complex spectrum is given by

$$I(x) = \int_0^\infty B_\sigma [1 + \cos\{8\pi(\sigma - \sigma_o)x\tan(\theta)\}]d\sigma \quad (3)$$

where B_σ is the input spectral signal at wavenumber σ. A Fourier transform of the interference pattern recovers the power spectrum of the input signal [2,3].

The fringes themselves are observed as a virtual image located at a position related to the optical path length and the dispersion of the grating. This relationship is given by

$$z = D \big/ 2\cos^2(\theta) \quad (4)$$

where z is the apparent distance behind either grating where fringe localization occurs, D is the path length through one arm of the interferometer and θ is the diffraction angle [2].

A missing element in the basic pattern is *color*. Equations 2 and 3 provide no differentiation in the fringe frequency represents a wavenumber that is bluer or redder than σ_o. In effect, it samples the absolute value of the wavenumber offset, or $|\sigma - \sigma_o|$. This would appear to be a significant problem, but it is addressed by slightly tilting one grating perpendicular to the plane of interference. A rotation of the grating by a small angle $\phi/2$ results in a small angle shift to the wavefront in one arm of the interferometer relative to the other. The result is a vertical fringe frequency $f_y = \phi\sigma$. In a complex spectrum of multiple signals the output intensity function then contains 2 dimensional interference pattern with an intensity described by

$$I(x,y) = \int_0^\infty B_\sigma [1 + \cos\{8\pi(\sigma - \sigma_o)x\tan(\theta)\} + \sigma y\phi]d\sigma \quad (5)$$

where y is the direction in the fringe localization plane perpendicular to the interference axis [2]. The introduction of the y frequency creates a rotation in the fringes that is related to the ratio of the f_x and f_y via

$$-f_x/f_y = \tan(\eta) = -4(\sigma - \sigma_o)\tan(\theta)/\phi\sigma \quad (6)$$

At $\sigma = \sigma_o$ the both f_x and η are 0. However, for $\sigma > \sigma_o$ we obtain $\eta < 0$, and for $\sigma < \sigma_o$ we obtain $\eta > 0$. Thus the *direction* of the tilt is related to whether the color is bluer or redder than σ_o [6].

2.1 Resolving Power and Étendue

The primary instrumental advantage of SHS is in its combination of high spectral resolution ($R = \delta\sigma/\sigma$) and large input acceptance angle (field of view-FOV) in a compact instrument. It is in this combination of characteristics that they differ most from the traditional grating spectrograph designs currently used for remote sensing on spacecraft. In a grating spectrograph, the spectral resolution is a convolution of the dispersive properties of the grating, the width of the field of view (which is re-imaged at the instrument focal plane) in the wavelength direction, and the "throw distance" between the grating and the detector. This convolution drives the spectral resolution *lower* if the size of the instrument is reduced and/or its FOV is increased. Thus, the typical high ($R>10^5$; 3 km/s) resolution spectrograph has a very narrow FOV, is quite large, and is employed at the focus of a large telescope (e.g. the HST-STIS Echelle), while the typical low-resolution spectrograph on a remote probe (e.g. Cassini UVIS) is compact, has a wide FOV, and *low* ($R<1000$; 300 km/s) spectral resolution.

A SHS is far better suited for applications requiring a compact, high-resolution instrument, particularly if the target is angularly extended. SHS instruments are not completely insensitive to the input FOV, but are far less so than grating designs. To first order this allows the instruments to sample the full theoretical resolving power of the grating, which is given by

$$R = 4\,W\,\sigma\sin\theta \quad (7)$$

where W is the illuminated width of the grating [2,3]. It is clear from this equation that resolution can become extremely high as the illuminated area of the grating increases or if the instrument is used in the UV. For example, a SHS using a first order grating with a 25° dispersion angle at 150 nm has a resolution *R~113000* when only 1 cm is illuminated. Indeed, a potential difficulty with SHS instruments is keeping the resolution *low* enough that a usable bandpass (see below) can be sampled. However, it also means that the size of the gratings, other optics, and the instrument housing will be small. Typical designs [2,4,5,6,7] illuminate no more than a few cm of a grating.

While the FOV of a SHS is far greater than that of a comparable resolution grating spectrometer, there is still a limit related it. In this case the limit comes from the dispersive properties of the grating. Only those rays at the tuning wavenumber and at the center of the field correspond to the Littrow configuration, with all other rays following different conditions where $\alpha \neq \beta$. From the perspective of the optical system changes in color *or* incoming angle will result in wavefront rotation relative to the tuning condition and thus the production of

fringes, such even for monochromatic light there is a 'lineshape' defined by the convolution of the theoretical resolving power and a pseudo 'chromatic spreading' across the FOV. The limit of this process is the point at which this spreading accumulates to one fringe of resolution across the spatial field. Beyond this point any increases in FOV destroy the fringe contrast from the edges of the spatial field inward, which have the same effect as reducing the resolution and the effective width (W) illuminated on the grating. It can be shown that this limit results in a maximum input solid angle of $\Omega=2\pi/R$ steradians, which is still several orders of magnitude larger than typical echelle grating systems [2,3]. In the UV SHS example above, the instrumental FOV is 0.2 sq°.

The interplay of resolution and FOV provide a third significant advantage of the SHS technique, its very large étendue. Étendue is defined as the product of the FOV and collecting area of an instrument ($\acute{E} = A_{eff} \times \Omega$), but more specifically it is a measure of the light gathering power of an instrument to a target that fills the FOV. The SHS maximizes its étendue through its input acceptance angle rather than with its collecting area, which means it will outperform echelle spectrometers on extended targets even when they are mounted to large telescopes. An illustrative example is the case of the echelle mode of HST-STIS using the recommended 0.2" x 0.2" aperture at R > 10^5. Coupled with the HST 2.4m aperture, this configuration had an étendue of É= 1.35 x10^{-4} cm^2-sq°, whereas our sample instrument has É = 0.2. Thus, for an aperture-filling target, our sample SHS instrument is *~1500 times more sensitive*.

2.2 Bandpass and Noise

The primary limitations of the basic SHS implementation come from its sampled bandpass and the manner in which spectral and detector noise is accommodated. As noted in equations 2 and 3 above, the output fringe frequency at the imaging plane is directly related to the separation from the tuning wavelength. In theory this can be any frequency, but in practice the maximum fringe frequency that can be sampled is determined by the number of pixels in the detector. In the best-case scenario (the Nyquist limit), the maximum number of fringes that can be sampled is half the number of pixels in the horizontal direction. Thus, a 2000 element array is necessary to detect 1000 fringes. In our example UV SHS with R~113000 at 150 nm each ±1 change in fringe frequency corresponds to one wavelength resolution element of 0.0013 nm such that sampling 1000 fringes would cover 1.3 nm of bandpass. In order to record those fringes however, they must be resolvable at the detector. Including the color effect produced with vertical cross-tilt (eqns. 5, 6) doubles this, with the caveat that the rotation of the fringes degrades the maximum frequency slightly from the Nyquist limit. In this case, our sample system has *at most* a 2.6 nm bandpass that is adequate only for a targeted instrument sampling a single line or molecular band.

Behind the bandpass limitation is a second, important mitigating factor in SHS design consideration. Light that is too far from the tuning wavelength to be resolved into fringes is *not* lost to the system, but reaches the detector as background noise. This signal becomes an important element of the data quality, because it is counted along with resolved spectral data in the transformed power spectrum. The signal to noise of a resolved component in an isolated emission line (S_λ) observed with a SHS is given by

$$\frac{s}{n}(\lambda) = \frac{S_\lambda \sqrt{t}}{\sqrt{S_{tot}}} \qquad (8)$$

where S_{tot} is the *total* signal obtained from the detector, including all resolved spectral elements, unresolved out of band signal, and detector dark and read noise [2,3]. This circumstance represents a mitigating limitation of SHS, which is that the *entire* spectrum contributes to each element of the interference pattern. This is as opposed to dispersive spectrographs where the s/n of each element is described by its own photon statistics and the statistics of the underlying continuum. This rather limits the sensitivity of SHS in cases with substantial background stellar continuum, where detector noise is significant, when large numbers of lines are detected, or for cases of high line intensity contrast (e.g. isotopic ratios).

Of the above noise sources, both out of band and detector signals can be mitigated by using an input band selection filter and a low-read/dark noise detector system. Additionally, making observations in the UV, where stellar continuum becomes weak can eliminate underlying signal within a filter bandpass.

3 ALL-REFLECTIVE SHS

The TGI (or beamsplit) configuration of the SHS has heritage in observations of airglow [4] and interstellar medium emissions [5,9], however there are alternative designs that offer properties that are potentially attractive for spaceflight and/or broadband applications. Our particular focus has been on the all-reflective version of the SHS [3,6,7]. All-reflective SHS instruments are configured similarly to a 2-mirror Sagnac Interferometer (fig. 2) where a single grating acts as both the dispersing element and a beamsplitter. Light in both arms travels the same optical path, but in opposite directions. This design has several positive

aspects making them attractive. Foremost is the lack of any requirement for refractive optics. This allows the reflective systems to be used over a wide wavelength range extending from the far and extreme UV to the near IR. In addition the reflective systems can be more robust. Unlike the beamsplit version described above, the optical path in the reflective system is such that light in both arms of the interferometer encounters all of the optical elements of the system following an anti-symmetric path. This makes the design self-compensating, because small changes in one optic affect both beams. Indeed, the stability and robustness of the Sagnac configuration has lead to their common use in laser gyros, which have substantial heritage in spaceflight and other challenging environments. This combination of characteristics also make them extremely useful for broadband systems, since their theoretical wavelength response covers a wide range and their design permits retuning without having to move a grating (see below).

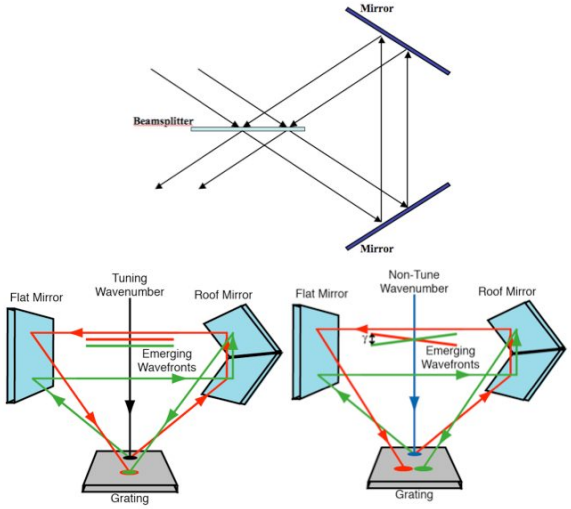

Fig. 2. At top is a two-reflection Sagnac configuration where the incoming beam is split, with both components following the same optical path in different directions. The beams recombine and exit. In the reflective SHS (a), the wavefronts at the tuning wavelength emerge parallel, while the wavefronts at a different wavelength (b) are rotated relative to each other at the output. Where the path difference between the two beams in (b) are equal to an integer multiple of the wavelength positive interference occurs.

4 TUNABLE SHS (TSHS)

A TSHS is optically identical to the single-line version of the instrument, except that it exploits the dependence of the tune on mirror/grating location to scan across wavelength. Consider the reflective SHS in figure 3. From equation 2 we see that the output fringe frequency is dependent on the cross-tilt γ between the wavefronts. A single *tune* of the instrument is defined as where $\gamma=0$, and this is set by rotating the flat and roof mirrors in the arms of the interferometer. Thus, if the mirrors are rotated anti-symmetrically from this angle, then the grating dispersion angle (θ) where $\gamma=0$ will change, resulting in (via eqn. 1) a change in σ_o (fig. 3). If the diffracted beam at the new σ_o is not vignetted in the optical path, then rotating the mirrors has set the instrument to a new tuning wavenumber.

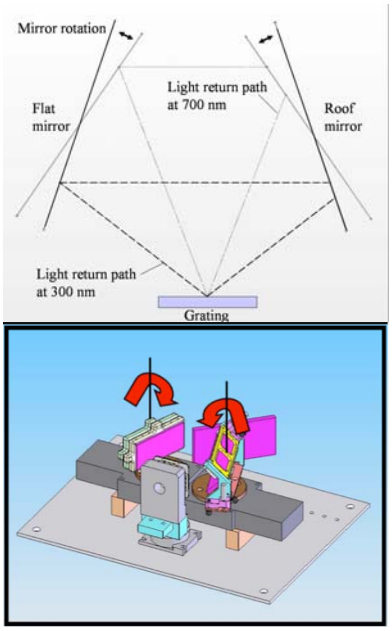

Fig 3. Top shows how rotation of the mirrors in the optical system can adjust the tuning wavenumber. Below a mechanical model of TSHS shows how such a design would be implemented.

A re-tunable SHS can cover a very a wide bandpass because the range of angles over which the mirrors in a SHS must rotate is typically very small per unit wavelength. The technical challenges are in the precision with which the rotation can be made, the larger size of the optics required, since the beam moves across the transfer mirrors as the dispersion angle changes, and the presence of any hysteresis introduced by rotating back and forth across the tuning range. In addition the location of fringe localization will change significantly as both the optical path and dispersion angle will be dependent on wavenumber via eqn 4 above. Finally there is the caveat that a series of filters is required to limit the input spectrum to the range of frequencies being targeted by each tune. The practical effect of this last point is similar to the requirement of an order separation filter in an echelle spectrograph. However, if the full usable bandpass it to be exploited the number of filters must be very large.

Our prototype TSHS instrument is shown in figure 4 with parameters described in table 1. The two interferometer mirrors are mounted on computer controlled high-precision (0.0005^o accuracy) motorized

rotation stages that be repositioned to complete the symmetric interferometric triangle determined by the diffraction angle (θ) associated with any wavelength of interest (see Fig. 3). Once the mirrors are positioned to a particular wavelength tune, they remain stationary until re-tuning to a different spectral region. No scanning or other motion is required to make an observation at a particular wavelength. As can be inferred from Fig. 3, the instrument's usable wavelength range is limited by the physical length of the mirrors and the diameter of the collimated beam. In our instrument a 15mm beam (W = 15mm) gives a theoretical range of 300 to 700nm. In principle, this system could be built for a wider usable range, extending further into the UV for example, simply by employing longer mirrors or by changing the grating to one with a different groove spacing.

Grating Groove Density	1200 gr/mm
Illuminated Width	12 mm
Theoretical Resolving Power	53000
Field of View	0.29°
Field Lens Focal Length (f.l.)	2000 mm
Collimating Lens f.l.	750 mm
Magnification Lens f.l.	1000 mm
Camera Lens	300 mm
CCD Model	Andor DU432-BU2
CCD Format	1024^2 (13μ pixels)

Table 1. The characteristics describing the prototype TSHS, including input and output optics coupling the instrument to the McMath-Pierce telescope and the Andor CCD.

The current implementation does present compromises. This system contains several transmissive elements for design simplicity, but the lenses' indices of refraction change with tune wavelength, varying their effective focal lengths. Achromatic lenses nearly eliminate this undesirable effect, but are not as transmissive in the near-UV (< 4000ºA) as fused silica singlets. A truly "all-reflective" system would eliminate this problem, but such a system would require further development of custom off axis input and output mirrors. The existing design requires that achromats be exchanged for singlets when operating in the UV to reduce attenuation. To account for movement in the fringe localization plane, the imaging optics at the output must be adjusted accordingly with every new tune to maintain good fringe focus and to properly magnify the pattern onto the largest possible number of CCD pixels. The output optics and camera are mounted on a slider-rail system to accommodate these adjustments. Finally, the off-the-shelf diffraction gratings used in the instrument are limited by their blaze function to a subset of the tuning range. Therefore, to operate effectively across the entire possible range, it is necessary to alternate between gratings optimized for the red and the blue.

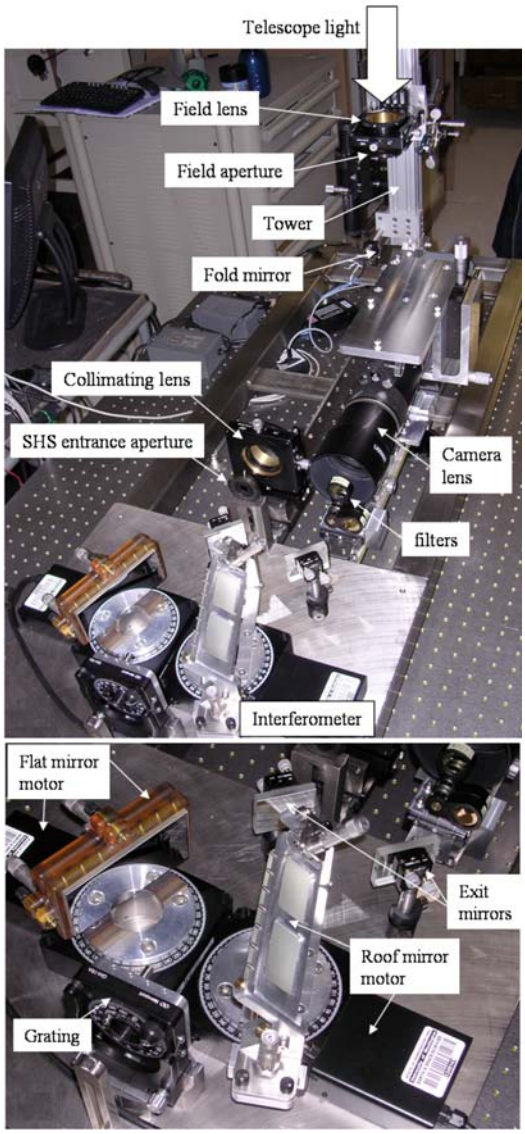

Fig. 4. At top is the full prototype assembly of the TSHS as it was used at the McMath-Pierce Solar Telescope at the Kitt Peak National Observatory. Below is a closeup of the instrument without the coupling optics.

5 FIRST LIGHT TESTING

The first-light observations of the variable-tune SHS were taken in June 2007 at the East Auxiliary port of the McMath-Pierce solar telescope, Kitt Peak National Observatory. This telescope tracks the ecliptic with a heliostat and focuses its f/50 beam at a spatially-fixed focal plane coincident with the entrance aperture of the SHS. This arrangement allows the instrument to be fixed onto a stationary surface directly below the telescope port. As shown in Fig. 4 (top), the SHS is coupled to the telescope's optical axis via a vertical tower, to which are affixed two apertures, used to both define the optical axis of the SHS during laser-alignment and to ensure during the collimation procedure that the telescope's optical path is co-axial

with the TSHS. A mirror folds the vertical beam into a horizontal plane for entry into the interferometer. One of the two apertures on the tower is the field aperture, placed at the telescope's focal plane to limit the instrument's accepted field of view, as discussed above in Sec. 2. Also at the focal plane is a field lens, which focuses an image of the telescope's primary mirror inside the interferometer, ensuring that the sky be completely de-focused near the fringe localization plane. The beam allowed through the field aperture passes through a collimating lens and another aperture of diameter *W* (the grating width to be illuminated) at the entrance of the interferometer. The imaging optics in this setup consisted of two lenses and an appropriate narrow-band filter positioned between them. The first lens along the output axis re-imaged the fringe plane to a distance accessible to the camera lens, a standard 300mm telephoto. As the distance to the fringe localization plane varies with wavelength, so does the magnification. In its current form the prototype lens positions had to be adjusted manually after each re-tuning of the instrument and the best magnification match to the CCD varied as a function of wavelength.

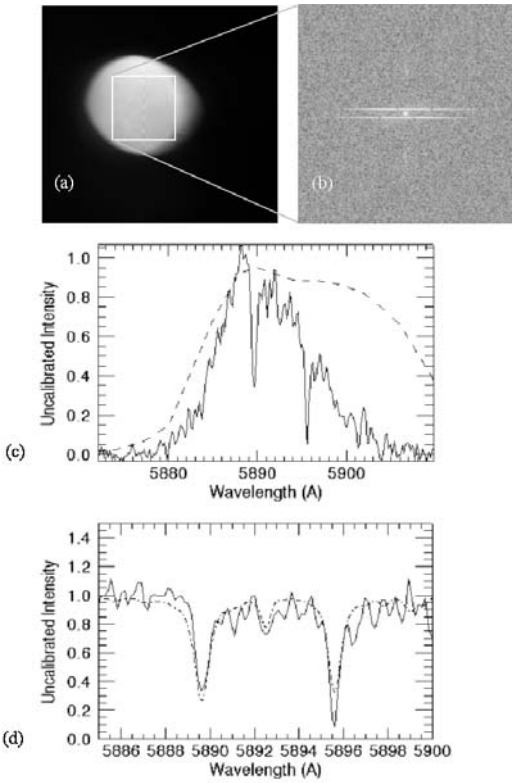

Tests of the instrument included observations of several lamps, then the day sky, and finally of an extended target, Jupiter (fig. 5). Blind tuning of the rotation stages robustly obtained spectral lines in the bandpass without significant hysteresis. In figure 5 the steps of the analysis are shown from the interference pattern to power spectrum to a spectrum of reflected solar continuum that could be matched to the existing catalog of solar Fraunhofer lines. As can be seen in the final spectrum we are able to recover the major lines in our bandpass in only a few seconds of integration time at a resolution (R~40000) close to the theoretical limit. One as yet unexplained characteristic of the instrument was its apparent loss of fringe contrast for light redward of the tuning wavelength (fig. 4c). This corresponds to a loss of a rotation direction in the interference pattern that was seen in test spectra and appeared to worsen as targets became more extended and the tuning wavelength increased to the red end of the spectral range. In its current form, the instrument has not been fully corrected for fringe distortion caused by variable flatness in the mirrors or grating or for diffractive effects in the lenses. It is likely that this is playing a role in the observed performance of the system.

6. CONCLUSIONS and FUTURE WORK

Based on the results of our initial testing the concept of TSHS appears to be robust and relatively easily achievable. Our prototype was able to approach the theoretical resolving power limit on astronomical targets over a range from 350-600 nm, with the precision rotation technique reliably acquiring target wavelengths separated by up to several hundred nm. Future work to eliminate refractive elements in the input/output optical train and to automate the output focusing of the fringe localization plane on to the detector will improve the efficiency with which the instrument can by dynamically tuned.

7. REFERENCES

1. Kruger R. A., Anderson L. W., and Roesler F. L., *Journal of the Optical Society of America*, Vol. 62, 938-945, 1972.
2. Harlander, J. M., *Ph.D. Thesis University of Wisconsin*, 1991.
3. Harlander J., Reynolds R. J., and Roesler F. L., *Astrophysical Journal*, Vol. 396, 730-740, 1992.
4. Harlander J. M., et al., *Applied Optics*, Vol. 41, 1343-1352. 2002.
5. Watchorn S., et al., *Proc. SPIE*, Vol. 4498, 284-295, 2001.
6. Harris W. M., et al., *Journal of Electron Spectroscopy*, Vol. 143, 973-977, 2005.
7. Stephan S. G., et al., *Astrophysical Journal*, Vol. 559, 491-500, 2001.
8. Mierkiewicz E. J., et al., *Proc. SPIE*, Vol. 5492, 751-766, 2004.